ELSEVIER

Physica A 238 (1997) 225–244

PHYSICA A

Accumulation points in nonlinear parameter lattices

Marcus W. Beims[a,1], Jason A.C. Gallas[a,b,2]

[a] *Instituto de Física, Universidade Federal do Rio Grande do Sul, 91501-970 Porto Alegre, Brazil*
[b] *Höchstleistungsrechenzentrum, Forschungszentrum Jülich, D-52425 Jülich, Germany*

Received 21 October 1996

Abstract

In 1963 Myrberg determined a period-doubling cascade of the quadratic map to accumulate at 1.401155189... As found later, the geometric way with which model parameters approach this value has universal behavior and several characteristic exponents associated with it. In the present paper we discuss the existence of an infinite number of points characterized by the simultaneous accumulation of two or more bifurcation cascades. We present an accurate numerical determination of the vertices of a doubly infinite nonlinear lattice which lead to a point of double accumulation. In addition, we discuss the number-theoretic nature of irrationalities characterizing vertices. Novel classes of universality with characteristic exponents are conjectured to exist near points of multiple accumulations.

PACS: 05.45.+b; 02.10.Gd; 02.10.Nj

1. Introduction

A recent paper in this Journal has shown that the parameter space of dynamical systems contains generically an infinite quantity of certain nonlinear lattices [1]. Such lattices appear whenever there is an intersection of families of curves, more precisely *varieties*, delimiting domains of stable physical behaviors. Since dynamical systems are well known to contain many different bifurcation cascades, whenever these cascades intersect (i.e. coexist), they produce a nonlinear lattice in parameter space. One example of a nonlinear parameter lattice is shown schematically in Fig. 1.

The lattice seen in Fig. 1 (which is a realistic blow-up of the parameter space of the Hénon oscillator defined in Eq. (2) below) results from the coexistence of two infinite

[1] E-mail: mbeims@if.ufrgs.br.
[2] E-mail: jgallas@if.ufrgs.br.

PII S0378-4371(96)00451-7

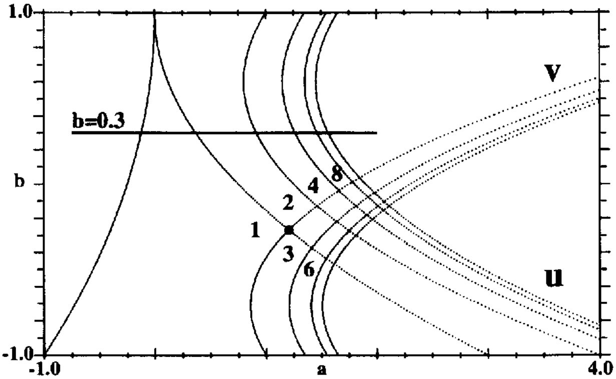

Fig. 1. Two families of parabolic-like arcs, u_k and v_j, delimiting regions of stable periodic motions of periods 1×2^m and 3×2^n, respectively. The black dot indicates the point of intersection of u_1 and v_1. Numbers represent the periodicity inside the region. For a more detailed picture see Fig. 3 in Ref. [1].

period-doubling cascades of stable motions beginning with the lowest possible periods: a period 1×2^m cascade and a period 3×2^n cascade. The letter $\mathbf{u}=\{u_1,u_2,\dots,u_\infty\}$ denotes collectively the family $\{u_j\}$ of curves which delimit domains of stability belonging to the 1×2^m cascade. Similarly, $\mathbf{v}=\{v_1,v_2,\dots,v_\infty\}$ denotes curves separating stability domains belonging to the 3×2^n cascade. Each family contains an infinite number of curves. The intersection of these two families of parabolic-like arcs defines a mesh of points, "vertices", a doubly infinite sequence of points. The parameter values defining each of these vertices are special in that they belong simultaneously to *three* different domains of stability, i.e. three different stable motions coexist for each vertex. The overlap of several bifurcation cascades as shown in Fig. 1 is a very common phenomenon in realistic dynamical systems.

The coordinates of the first few vertices were determined analytically in Ref. [1], with the interesting result that parameter values defining such vertices are invariably *units* or simple functions of units in specific algebraic number fields.

The units of a system of algebraic integers are those algebraic integers whose reciprocals are also algebraic integers [2]. For example, the first intersection point of the nonlinear lattice shown in Fig. 1 (the black dot in the figure) is the point $p_{1,1}$ with coordinates

$$p_{1,1}: \quad (a_{1,1},b_{1,1}) \equiv (-\tfrac{9}{2}\xi,\xi)\,, \tag{1}$$

where the number $\xi=-2+\sqrt{3}$ is a unit in the real quadratic field $\mathbf{Z}(\sqrt{3})$ because its reciprocal, $\xi^*=1/\xi=-2-\sqrt{3}$, is an integer in the same field. Notice that $\xi\xi^*=(-2+\sqrt{3})(-2-\sqrt{3})=1$. The product of a *quadratic* unit and its reciprocal (the so-called "norm" of the unit) is always equal to either $+1$ or -1. Thus, the norm of units can be either positive or negative.

The fact that bifurcation points belonging to overlapping cascades involve units in their definitions seems to indicate that without too much difficulty it should be possible to find analytic expressions for the specific towers of algebraic numbers characterizing the cascades. If one succeeds in learning about the number-theoretic symmetries behind specific towers of numbers involved in bifurcation cascades, one will have opened the door to the analytic computation of scaling properties, in general, for these systems.

While it is not difficult to recognize the presence of specific towers of algebraic numbers, their explicit determination (even for cascades with the lowest possible periods like 1×2^m and 3×2^n) is far from trivial. An indication of the difficulties involved might be obtained by noticing that while the properties of quadratic number fields are essentially known since the middle of the last century, cubic number fields are still today object of active research. Results for number fields of higher degrees exist only for a few specific cases. See, for example, Refs. [3–5] and references therein.

The present paper, which might be considered an extension of Ref. [1], serves two different purposes. The principal purpose is to obtain precise numerical approximations for the locations of several vertices forming the nonlinear lattice. These parameter values are required as input for number-theoretic procedures aiming to uncover the analytical characteristic of the algebraic numbers composing the lattice. A preliminary use of these precise values is made at the end of the paper, where we discuss certain "linear dependences" involving parameters. Accurate parameter values are also important to understand the exact nature of the sequence of orbits ruling the dynamics observed in sets living on the basin boundaries in phase space when the periodicity increases without bounds [6].

As a secondary purpose we use our accurate parameters to obtain as a by-product some metric properties of bifurcation cascades depending simultaneously on two parameters. Notice that while it is possible to find interesting papers in the literature discussing methods for the accurate determination of bifurcation parameters, systematic results derived from such methods do not seem to exist [7,8]. We emphasize that an accurate determination of long sequences of bifurcation parameters is a prerequisite for the determination of number-theoretic relationship between different points in parameter space.

2. Nonlinear lattices of parameters

In this section we define more precisely the subject of our main interest, namely the nonlinear lattice of parameters shown schematically in Fig. 1. Lattices like this are seen commonly in dynamical systems but for definiteness we will present results for one of the standard models in dynamics, the Hénon oscillator, which is defined by the equations

$$x_{t+1} = a - x_t^2 + b y_t, \qquad y_{t+1} = x_t . \tag{2}$$

Recall that one of the lessons that has emerged from the study of nonlinear systems in recent years is that most properties found in these systems have a large degree of universality. In other words, the particular system chosen for study, within wide limits, seems to be relatively irrelevant.

The lattice in Fig. 1 is formed by the intersection of the two bifurcation cascades which start with the lowest possible periodicities: 1×2^m and 3×2^n. The black dot denotes the intersection $p_{1,1}$ of the pair of curves (more precisely, algebraic varieties) defined by the equations

$$u_1: \quad -4a + 3 - 6b + 3b^2 = 0 \quad \text{(bifurcation } 1 \to 2\text{)}, \tag{3}$$

$$v_1: \quad -4a + 7 + 10b + 7b^2 = 0 \quad \text{(birth of period 3)}. \tag{4}$$

This pair of varieties defines the two leftmost boundaries of the nonlinear lattice.

Adjacent to u_1 and v_1 one finds the varieties characterizing the next bifurcations in both cascades. Such varieties are defined by the equations

$$u_2: \quad -4a + 5 - 6b + 5b^2 = 0 \quad \text{(bifurcation } 2 \to 4\text{)}, \tag{5}$$

$$\begin{aligned} v_2: \quad & 64a^3 - 32(4 + b + 4b^2)a^2 + (72 - 216b - 252b^2 - 216b^3 + 72b^4)a \\ & -81 - 54b - 18b^2 + 90b^3 - 18b^4 - 54b^5 - 81b^6 = 0, \\ & \text{(bifurcation } 3 \to 6\text{)}. \end{aligned} \tag{6}$$

The expressions for u_1 and u_2 are well-known. Those for v_1 and v_2 were obtained recently [1], after relatively long algebraic manipulations. [3]

As might be recognized from Fig. 1, the nonlinear lattice is delimited by four varieties: u_1 and v_1, as mentioned above, and, additionally, by u_∞ and v_∞, where

$$u_\infty = \lim_{j \to \infty} u_j \quad \text{(accumulation of the } 1 \times 2^m \text{ cascade)}, \tag{7}$$

$$v_\infty = \lim_{j \to \infty} v_j \quad \text{(accumulation of the } 3 \times 2^n \text{ cascade)}. \tag{8}$$

The varieties u_∞ and v_∞ are defined by those parameters for which aperiodic (i.e. "chaotic") motion appears for the *first time* while bifurcating along the cascades 1×2^m and 3×2^n, respectively. While all points lying on varieties u_j and/or v_j having *finite* values of j imply parameters and orbits defined necessarily by *algebraic* numbers, points lying on u_∞ and/or v_∞ require the existence of units characterized by *transcendental* numbers. Thus, as discussed in Ref. [1], parameter values defined by transcendental units seem to be the number-theoretic hallmark characterizing the precise location of the transition from periodic to aperiodic, "chaotic", motions in phase space.

Ideally, one would like to derive analytical expressions for all varieties v_j and u_k, for $j, k = 1, 2, \ldots, \infty$ and, from them, to extract exact coordinates of all intersection points $p_{j,k}$ embedded in the lattice. This is a quite difficult task. In spite of this, the many symmetries displayed [1] (see also Refs. [9,10]) by the numerical values defining the coordinates of the intersection points make it plausible to hope to find sequences of

[3] Note added in proof: We found recently that the analytical expression for v_j was already known to D.L. Hitzl and F. Zele, in: An exploration of the Hénon quadratic map, Physica D 14 (1985) 305–326.

analytical expressions within suitable towers of number fields, sequences that should allow one to take the limit of period length going to infinity analytically. It would be very nice, of course, to obtain the towers of numbers parametrically, i.e. as an explicit function of the physical parameters of the model.

Notice that the algebraic varieties discussed in this section are defined physically in parameter space as *the frontiers between domains of stable motions of different periodicities*. Since generically such frontiers are very seldom straight lines, the more realistic situation in models involving more than one parameter is to consider bifurcation cascades occurring under the simultaneous variation of such parameters, a new and slightly more complicated situation.

3. Accumulation points of single cascades

Before considering simultaneous points of accumulation for two bifurcation cascades, we start by reconsidering briefly the points of accumulation for two bifurcation cascades of great practical and historical relevance: (i) the cascade for $b=0$, considered earlier by Myrberg [11,12], and (ii) the cascade for $b = 0.3$, considered earlier by Derrida et al. [13] (see also Refs. [14,33]). The purpose of this is to compare our numbers with those available in the literature as well as to produce numbers which will appear below as limiting cases of a more general setting.

When $b=0$ in Eq. (2) the dynamics of x and y is the simplest possible: x is ruled by the *quadratic map* $x \mapsto a - x^2$ while y simply lags x by one time step. Thus, the dynamics observed when measuring any one of the variables is simply that corresponding to the one-dimensional quadratic map. Notice, however, that even for $b = 0$ the Hénon map remains a two-dimensional system.

The dynamics of a quadratic map was considered almost 40 years ago by Myrberg in a remarkable series of papers reporting calculations done already with a computer (with an *Elektronenmaschine*, as he writes). Myrberg used the essentials of what is presently known under the name of "symbolic dynamics" [34,35] applying it in practice to extract with remarkable numerical accuracy (10 decimal places), among other results, the accumulation point of the 1×2^m cascade for the quadratic map. Myrberg reports [12] this accumulation point ("der Endpunkt des Spektrums") to be located approximately at

$$\text{Myrberg point}: \quad (a,b) = (1.401155189\ldots,0.0)\,. \tag{9}$$

Table 1 presents our results for the first 26 "superstable points" [13] calculated using a slightly modified version of the computer program given in Ref. [15]. These superstable points happen to be the same points used previously by Myrberg [12] in the definition of his "Nullzyklen" (see also Ref. [16]). The work of Myrberg is cited in the epoch-making paper of May [36]. It is discussed quite passionately in the inspiring book of Mira [16]. Table 1 displays also the characteristic geometric

Table 1
Superstable points for the quadratic map $x_{t+1} = a - x_t^2$. The symbol ∞ refers to an extrapolated value. See text

m	2^m	a	δ_m^a
0	1	0.0	
1	2	1.0	3.2185114220380
2	4	1.310 702 641 336 832 883 563 570 797	4.3856775985683
3	8	1.381 547 484 432 061 469 540 693 562	4.6009492765380
4	16	1.396 945 359 704 560 641 672 477 987	4.6551304953919
5	32	1.400 253 081 214 782 797 325 012 282	4.6661119478285
6	64	1.400 961 962 944 841 040 296 116 315	4.6685485814468
7	128	1.401 113 804 939 776 123 900 879 658	4.6690606606482
8	256	1.401 146 325 826 946 178 647 288 239	4.6691715553795
9	512	1.401 153 290 849 923 881 474 672 291	4.6691951560300
10	1024	1.401 154 782 546 617 841 218 612 538	4.6692002290868
11	2048	1.401 155 102 022 463 975 894 064 914	4.6692013132942
12	4096	1.401 155 170 444 411 263 765 357 879	4.6692015457809
13	8192	1.401 155 185 098 297 290 530 984 480	4.6692015955374
14	16384	1.401 155 188 236 710 941 543 786 461	4.6692016061981
15	32768	1.401 155 188 908 863 038 563 264 270	4.6692016084808
16	65536	1.401 155 189 052 817 434 492 244 661	4.6692016089697
17	131072	1.401 155 189 083 648 057 794 617 719	4.6692016090744
18	262144	1.401 155 189 090 251 033 181 770 570	4.6692016090969
19	524288	1.401 155 189 091 665 188 307 196 808	4.6692016091015
20	1048576	1.401 155 189 091 968 057 029 478 934	4.6692016091002
21	2097152	1.401 155 189 092 032 922 235 061 798	4.6692016091126
22	4194304	1.401 155 189 092 046 814 375 734 471	4.6692016090573
23	8388608	1.401 155 189 092 049 789 646 848 429	4.6692016089171
24	16777216	1.401 155 189 092 050 426 858 809 522	4.6692016103177
25	33554432	1.401 155 189 092 050 563 330 098 251	
∞	∞	1.401 155 189 092 050 600 523 82	

scaling [17–20]

$$\delta = \lim_{\ell \to \infty} \delta_\ell, \quad \text{where } \delta_\ell \equiv \frac{a_\ell - a_{\ell-1}}{a_{\ell+1} - a_\ell}, \tag{10}$$

of one-dimensional systems. The last line in Table 1 shows an extrapolated value, in an attempt to guess the location of the accumulation point marking the "end point of the cascade". Here and in similar tables below, extrapolated values were obtained (from the last three parameter values shown in the tables) using the δ^2 process described by Todd [21] which, according to him, has been popularized in numerical analysis by Aitken, Shanks and others during this century, but dates back at least to Kummer in 1837. This δ^2 process has nothing to do with the δ in Eq. (10), at least as far as we can see.

Comparing Eq. (9) and Table 1 one sees that there is perfect agreement between the accumulation value calculated by Myrberg [12] and the new one being reported here.

Table 2 shows results analogous to those in Table 1, but for $b = 0.3$ now (see Fig. 1). It contains also a comparison between our numbers and those calculated by

Table 2
Comparison of bifurcation points along the line $b = 0.3$ with those reported by Derrida et al. [13]

m	1×2^m	$a_{present}$(top) and a_{DGP}(bottom)	δ_m^{DGP}	$\delta_m^{present}$
0	1	−0.122 5		
		−0.122 5		
1	2	0.367 5		0.89908256880
		0.367 5		
2	4	0.912 5		4.80788719025
		0.912 5	4.844	
3	8	1.025 855 405 073 781 052		4.48572427447
		1.026	4.3269	
4	16	1.051 125 662 035 171 236		4.64689413113
		1.051	4.696	
5	32	1.056 563 758 158 788 020		4.65956869798
		1.056 5(36)	4.636	
6	64	1.057 730 839 594 022 683		4.66732531586
		1.057 730 83	4.7748	
7	128	1.057 980 893 180 660 019		4.66875332603
		1.057 980 893 1	4.6696	
8	256	1.058 034 452 143 658 301		4.66911064458
		1.058 034 452 15	4.6691	
9	512	1.058 045 923 056 873 958		4.66918147101
		1.058 045 923 04	4.6691	
10	1024	1.058 048 379 785 807 469		4.66919737588
		1.058 048 379 80	4.6694	
11	2048	1.058 048 905 942 389 797		4.66920069257
		1.058 048 905 931		
12	4096	1.058 049 018 629 039 391		4.66920141394
13	8192	1.058 049 042 763 069 946 5		4.66920156718
14	16384	1.058 049 047 931 840 282 982		4.66920160019
15	32768	1.058 049 049 038 832 608 235 552		4.66920160718
16	65536	1.058 049 049 275 916 465 045 292		
∞	∞	1.058 049 049 340 531 02		

Derrida et al. [13]. As seen from the comparison in Table 2, apart from small differences in the last decimal places, the overall agreement between the numbers of Ref. [13] and the present ones is quite good. While recalculating the values given in Table 2 we noticed an inversion between two digits in the fifth bifurcation value reported by Derrida et al. [13]. This inversion, indicated by the parenthesis in Table 2, is responsible for the apparent maximum for $m=6$ in the convergence of their δ_m.

4. Points of multiple accumulations

This section reports an accurate numerical determination of the coordinates of a point in parameter space where two bifurcation cascades accumulate simultaneously. We begin by introducing a convenient notation to simplify the discussion to follow.

The particular points in parameter space where *two* bifurcation cascades accumulate simultaneously will be called points of *double* accumulation and will be denoted by $\mathscr{A}_{\kappa_1,\kappa_2}$ where κ_1 and κ_2 indicate the lowest possible periods characterizing each cascade. Since cascades starting with the lowest possible different periods are 1×2^m and 3×2^n, we have that the point of double accumulation with lowest possible nondegenerate indices is $\mathscr{A}_{1,3}$. When more than two cascades accumulate simultaneously one simply appends more sub-indices. It is possible to find in parameter space more than one point of double accumulation characterized by the same indices κ_1 and κ_2. However, since this situation will not be discussed presently, there is no necessity to overload the notation with extra indices here.

We determine the coordinates of $\mathscr{A}_{1,3}$ by computing coordinates for several vertices lying along specific directions in parameter space and studying how these coordinates evolve as the periodicity increases without bounds. The availability of exact expressions for the varieties u_1 and v_1 (see Eqs. (3) and (4)) make it not too difficult to compute vertices along these two directions. The computation of points of multiple accumulation involves generically tuning more than one physical parameter simultaneously.

Tables 3 and 4 present accurate coordinates for the first 16 vertices lying along the varieties v_1 and u_1, respectively. These tables also display extrapolated values aiming at guessing the coordinates a and b marking the point of double accumulation.

Comparing parameters values for last few vertices among themselves and with their extrapolated values one obtains a good idea of the speed with which one is approaching the end of the cascade and of the accuracy of the parameters. For example, all b values for vertices beyond the 12th in both tables have at least 5 correct decimal places. While this accuracy is certainly limited in absolute terms, it is well beyond the accuracy presently obtained experimentally in real physical systems [19].

As an additional byproduct, Tables 3 and 4 present some δ_ℓ values as defined in Eq. (10) above. As expected one finds no noticeable difference between the δ_ℓ sequences obtained along the varieties u_1 and v_1 and those obtained along the cut $b = 0.3$. This is due, in part, to the very high accumulation speed of the cascades. Notice that the limiting values obtained for δ seem to be independent of the parameter used to compute them.

Although the several scalings and limiting values of δ shown in these tables seem all to agree, any finite-precision computation prevents one from ruling out the possibility that real differences in the final limits do indeed exist. A definite answer to this question requires obtaining analytical expressions for the sequences of points, i.e. for the tower of algebraic numbers, characterizing bifurcations, a quite challenging task.

We now describe a numerical experiment devised to find the approximate location of a point of double accumulation in parameter space. The particular example discussed

Table 3
Vertices along the variety v_1, defined in Eq. (3). The symbol ∞ refers to an extrapolated value. See text

m	1×2^m	$a_{1,m}$ (top) and $b_{1,m}$ (bottom)	δ_m^a	δ_m^b
1	2	1.205 771 365 940 052 179		
		−0.267 949 182 431 122 706		
2	4	1.460 691 518 614 705 820	4.03309655299	
		−0.127 016 653 792 583		4.70001361011
3	8	1.523 898 572 878 143 334	4.41969063011	
		−0.097 031 094 104 990 76		4.55387553843
4	16	1.538 199 812 388 608 817	4.61432794102	
		−0.090 446 469 770 292 36		4.64408077140
5	32	1.541 299 123 857 853 781	4.65700859704	
		−0.089 028 616 666 778 63		4.66342832232
6	64	1.541 964 639 371 656 920	4.66661355162	
		−0.088 724 580 021 307 39		4.66799086482
7	128	1.542 107 251 462 082 084	4.66864369524	
		−0.088 659 447 793 272 81		4.66893878076
8	256	1.542 137 798 254 627 055	4.66908253250	
		−0.088 645 497 679 319 09		4.66914573579
9	512	1.542 144 340 609 004 454	4.66917605413	
		−0.088 642 509 956 351 53		4.66918959057
10	1024	1.542 145 741 788 634 766	4.66919614243	
		−0.088 641 870 075 937 68		4.66919904153
11	2048	1.542 146 041 878 754 686	4.66920043746	
		−0.088 641 733 033 072 69		4.66920105836
12	4096	1.542 146 106 148 884 859	4.66920135820	
		−0.088 641 703 682 684 21		4.66920149118
13	8192	1.542 146 119 913 579 341 5	4.66920155532	
		−0.088 641 697 396 729 632		4.66920158380
14	16384	1.542 146 122 861 555 418 225	4.66920159775	
		−0.088 641 696 050 470 649 46		4.66920160385
15	32768	1.542 146 123 492 921 619 706	4.66920160663	
		−0.088 641 695 762 143 201 29		4.66920160794
16	65536	1.542 146 123 628 140 925 847 94		
		−0.088 641 695 700 392 291 318 5		
∞	∞	1.542 146 123 664 993 44		
		−0.088 641 695 683 562 7		

Table 4
Vertices along the variety u_1, defined in Eq. (4)

n	3×2^n	$a_{n+1,1}$ (top) and $b_{n+1,1}$ (bottom)	δ_n^a	δ_n^b
0	3	1.205 771 365 940 052 179		
		−0.267 949 182 431 122 706		
1	6	1.232 588 541 359 191 903	2.37746301233	
		−0.281 971 680 061 194 853		2.39599377657
2	12	1.243 868 285 893 604 145	4.27424448656	
		−0.287 824 152 253 719 28		4.28624971215
3	24	1.246 507 289 013 305 654	4.58111243943	
		−0.289 189 558 864 175 54		4.58408115858
4	48	1.247 083 349 144 510 858	4.64939011431	
		−0.289 487 417 100 045 92		4.65004264877
5	96	1.247 207 249 294 216 748	4.66499935792	
		−0.289 551 472 047 143 86		4.66514005735
6	192	1.247 233 808 815 494 158	4.66829320428	
		−0.289 565 202 598 919 46		4.66832338078
7	384	1.247 239 498 158 497 082	4.66900797706	
		−0.289 568 143 815 852 32		4.66901444194
8	768	1.247 240 716 692 076 564	4.66916001931	
		−0.289 568 773 759 702 23		4.66916140398
9	1536	1.247 240 977 666 978 782	4.66919271636	
		−0.289 568 908 675 545 87		4.66919301291
10	3072	1.247 241 033 559 917 470	4.66919970289	
		−0.289 568 937 570 441 25		4.66919976640
11	6144	1.247 241 045 530 478 218	4.66920120033	
		−0.289 568 943 758 845 44		4.66920121393
12	12288	1.247 241 048 094 205 980 931	4.66920152229	
		−0.289 568 945 084 212 228 59		4.66920152520
13	24576	1.247 241 048 643 277 969 084	4.66920159036	
		−0.289 568 945 368 065 211 76		4.66920159098
14	49152	1.247 241 048 760 872 375 221	4.66920160498	
		−0.289 568 945 428 857 828 57		4.66920160512
15	98304	1.247 241 048 786 057 495 951 58	4.66920160836	
		−0.289 568 945 441 877 745 463 8		4.66920160839
16	196608	1.247 241 048 791 451 377 570 54		
		−0.289 568 945 444 666 212 952 9		
∞	∞	1.247 241 048 792 921 419 8		
		−0.289 568 945 445 426 178		

here is the point $\mathscr{A}_{1,3}$ for the Hénon map. The Hénon map contains just one double accumulation point with indices 1 and 3.

We started by calculating the values of a corresponding to the bifurcations 14, 15 and 16 for a few values of b, equally spaced by $\Delta b = 0.05$. For the cascade 1×2^m we considered the interval $-0.15 \leqslant b \leqslant 0.3$, while for the cascade 3×2^n the interval chosen was $-0.3 \leqslant b \leqslant 0$. From these three set of values we computed the extrapolated limit using the well-known δ^2 process [21]. Finally, to the extrapolated values we least-square-fitted a polynomial curve, producing the following approximations for the varieties $W^+_{1\times 2^\infty}$ and $W^+_{3\times 2^\infty}$

$$\begin{aligned} W^+_{1\times 2^\infty} = & -a + 1.4011551890920506 - 1.48961113368203419582\, b \\ & + 1.13805356609191002051\, b^2 + 0.00457532460749333865 93\, b^3 \\ & + 0.16769877512231015206 1\, b^4 - 0.01655852843780304310 04\, b^5 \\ & - 0.13439915342248621 98\, b^6 + 0.00531657267400575643 85\, b^7 \\ & + 0.11516420495387846433 2\, b^8 + 0.00917589514196271197 84\, b^9 \\ & - 0.03378519540020504978\, b^{10}, \quad -0.15 \leqslant b \leqslant 0.3\,, \end{aligned} \tag{11}$$

$$\begin{aligned} W^+_{3\times 2^\infty} = & -a + 1.77981807583499136 42 + 2.40551820628136011662\, b \\ & + 1.90576027714566027866\, b^2 - 0.17369532431943353426 6\, b^3 \\ & + 0.06397901666272588113 5\, b^4 + 0.05742784197460576740 8\, b^5 \\ & - 0.64542593292313477241\, b^6 + 0.05099500087904815513 6\, b^7 \\ & + 0.39567237258602803995\, b^8 - 0.42909097875424947066\, b^9 \\ & + 0.29375286243536933848 3\, b^{10}, \quad -0.3 \leqslant b \leqslant 0.0\,. \end{aligned} \tag{12}$$

For $b = 0$ one sees that the value of a obtained from $W^+_{1\times 2^\infty}$ agrees well with that in Table 1. The value in Eq. (11) was obtained from a fit, i.e. totally independent of the way in which the value in Table 1 was obtained. Thus, the number of correct digits of a for $b = 0$ in Eq. (11) gives an idea of the accuracy that we hope to have in all other coefficients.

Now, by equating $W^+_{1\times 2^\infty}$ and $W^+_{3\times 2^\infty}$ to zero one obtains the equations providing approximations for u_∞ and v_∞, respectively. The intersection of u_∞ and v_∞ gives, finally, the following approximate location for the point $\mathscr{A}_{1,3}$

$$\mathscr{A}_{1,3}: \quad (a_{\infty,\infty}, b_{\infty,\infty}) = (1.56012804937528, -0.099195603261691)\,. \tag{13}$$

Table 5
Coordinates of 17 vertices along the main diagonal

$p_{m,n+1}$	$a_{m,n+1}$	$b_{m,n+1}$
$p_{1,1}$	1.205771365940053	−0.267949192431122
$p_{2,2}$	1.474410762599143	−0.134526112591863
$p_{3,3}$	1.541043584260103	−0.106940716349456
$p_{4,4}$	1.556005301873558	−0.100862440058850
$p_{5,5}$	1.559243397607871	−0.099552999236862
$p_{6,6}$	1.559938507113985	−0.099272164788758
$p_{7,7}$	1.560087451694554	−0.099212001259090
$p_{8,8}$	1.560119354447116	−0.099199115257573
$p_{9,9}$	1.560126187194619	−0.099196355433690
$p_{10,10}$	1.560127650567009	−0.099195764362221
$p_{11,11}$	1.560127963976888	−0.099195637772734
$p_{12,12}$	1.560128031099702	−0.099195610661139
$p_{13,13}$	1.560128045475354	−0.099195604854666
$p_{14,14}$	1.560128048554122	−0.099195603611064
$p_{15,15}$	1.560128049213568	−0.099195603344762
$p_{16,16}$	1.560128049354789	−0.099195603287722
$p_{\infty,\infty}$	1.56012804937528	−0.099195603261691
$(p_{\infty,\infty} - p_{16,16})$	2.0491×10^{-11}	2.6031×10^{-11}

All digits in Eq. (13) are believed correct. We conjecture the dynamics measured near points of multiple accumulations to produce new classes of universality as well as new characteristic exponents.

Accumulation points analogous to $\mathscr{A}_{1,3}$ are generalizations of the accumulation point reported by Myrberg [11,12], although the number-theoretic issues related with such numbers were of no concern to him.

An additional interesting sequence of points on the lattice is the "diagonal sequence" $p_{\ell,\ell}$, i.e. the sequence defined by the intersection of the varieties u_ℓ and v_ℓ for all $\ell = 1, 2, \ldots, \infty$. This sequence starts with $p_{1,1}$, defined in Eq. (1), ending with $\mathscr{A}_{1,3}$, defined in Eq. (13). Accurate approximations to the first sixteen points of this sequence are given in Table 5. The accurate determination of diagonal points requires considerable investment of computer time due to the necessity of investigating limiting processes for *each parameter* involved in the process.

The nonlinear lattices leading to points of multiple accumulation involve nonhomogeneous compressions of more than one parameter. Therefore, as might be

Table 6
Two rows of off-diagonal vertices, one above and one below the main diagonal

$p_{m,n+1}$	$a_{m,n+1}$	$b_{m,n+1}$
$p_{3,2}$	1.480783754928471	−0.137988484966247
$p_{2,3}$	1.535559829218792	−0.103785572524048
$p_{4,3}$	1.542335882525508	−0.107682309952744
$p_{3,4}$	1.554755236308571	−0.100135908697606
$p_{5,4}$	1.556279318829526	−0.101021602877239
$p_{4,5}$	1.558971332926447	−0.099394537329761
$p_{6,5}$	1.559301941742203	−0.099587093413353
$p_{5,6}$	1.559880052647120	−0.099238102885625
$p_{7,6}$	1.559951039308359	−0.099279467200613
$p_{6,7}$	1.560074923614321	−0.099204700328724
$p_{8,7}$	1.560090135414580	−0.099213565228717
$p_{7,8}$	1.560116670915810	−0.099197551355911
$p_{9,8}$	1.560119929204602	−0.099199450212877
$p_{8,9}$	1.560125612445789	−0.099196020481503
$p_{10,9}$	1.560126310289461	−0.099196427170897
$p_{9,10}$	1.560127527472564	−0.099195692625157
$p_{11,10}$	1.560127676930127	−0.099195779726135
$p_{10,11}$	1.560127937613789	−0.099195622408826
$p_{12,11}$	1.560127969623060	−0.099195641063214
$p_{11,12}$	1.560128025453532	−0.099195607370659
$p_{13,12}$	1.560128032308939	−0.099195611365859
$p_{12,13}$	1.560128044266117	−0.099195604149945
$p_{14,13}$	1.560128045734279	−0.099195605005562
$p_{13,14}$	1.560128048295197	−0.099195603460167
$p_{15,14}$	1.560128048609644	−0.099195603643421
$p_{14,15}$	1.560128049158046	−0.099195603312405
$p_{16,15}$	1.560128049225447	−0.099195603351685
$p_{15,16}$	1.560128049342910	−0.099195603280799

recognized from Fig. 1, the "cells" composing the mesh of the lattice contain curved sides. In Table 6 we give two "off-diagonal" sequences of coordinates for the first few curved cells. These are the cells that, when the periodicity increases without limit, will "collapse" to form the vertex $\mathscr{A}_{1,3}$. It would be interesting to investigate the rate with which the area of such cells decreases as the periodicity increases without limit and to study what kind of universal behaviors exist for this generalized situation.

5. Digression on periodic representations of parameter values

It is not difficult to show that the polynomials generated by finite compositions of arbitrary polynomial equations of motion can always be solved in terms of finite chains of radicals. What is not so easy is to find these solutions explicitly, for specific dynamical systems. These solutions contain the physics and need to be obtained.

Several aspects of the nature of the difficulties involved in computing exact representations for the algebraic numbers defining vertices in parameter space and/or orbits in phase space are best explained by reference to definite examples.

In Ref. [1] it is shown that the intersection of v_1 and u_1 (the point $p_{1,1}$ in Eq. (1) here) may be written in three different forms:

$$\xi = -2 + \sqrt{3} = 1 - \sqrt{6}\sqrt{2-\sqrt{3}} = \left[-5 + \sqrt{6}\sqrt{38 - 21\sqrt{3}}\right] \Big/ 7 . \tag{14}$$

Similarly, that the intersection of v_1 and u_2 occurs at

$$p_{1,2}: \quad (a_{1,2}, b_{1,2}) \equiv (-\tfrac{23}{2}\eta, \eta) , \tag{15}$$

where η is the unit

$$\eta = -4 + \sqrt{15} = \left[3 - \sqrt{2}\sqrt{452 - 115\sqrt{15}}\right] \Big/ 5 = \left[-5 + \sqrt{2}\sqrt{632 - 161\sqrt{15}}\right] \Big/ 7 . \tag{16}$$

The difficulty is that it is not completely trivial to recognize that the representations of ξ and η on the right might be simplified to give the much simpler forms shown on the left. More technically, to recognize that ξ and η are *quadratic*, not *quartic* irrationalities. Even less obvious is to obtain, for example, the following simplified representation of the number θ, where

$$\begin{aligned} 64 \times \theta &= -4 + 4\sqrt{17} - (3 - \sqrt{17})\sqrt{170 + 38\sqrt{17} + 4\sqrt{\alpha_-}} \\ &\quad + 4\sqrt{6}\sqrt{68 - 4\sqrt{17} - (3-\sqrt{17})\sqrt{170 + 38\sqrt{17} - 4\sqrt{\alpha_+}}} , \\ &\simeq 64 \times 1.55816\ldots , \end{aligned} \tag{17}$$

where $\alpha_{\pm} \equiv 68 + 12\sqrt{17} \pm 4\sqrt{170 + 38\sqrt{17}}$. This point θ belongs to one of the total of 30 possible period-8 trajectories of the Hénon map. The particular analytical representation above is for $a=2$ and $b=0$. A point $\theta^* \simeq -1.93959\ldots$ belonging to the corresponding *conjugate* trajectory of period-8 is obtained by considering the negative branch in all square-root functions which appear in θ, i.e. by reverting signs in front of all the square-root functions which appear in θ.

Thanks to a well-known result [almost invariably attributed to Lagrange (1736–1813) but, according to Weil [22], already known to Euler (1670–1743) and in part even to Huyghens (1629–1695)], one knows that every quadratic algebraic number has a periodic representation in terms of continued fractions [23–25]. The first two bifurcations along the variety v_1 involve parameters which are simple functions of quadratic algebraic numbers. Their exact periodic representations may be easily determined:

$$\xi = -2 + \sqrt{3} = \{-1, 1, 2, 1, 2, 1, 2, \ldots\} \equiv \{-1, \overline{1, 2}\}, \tag{18}$$

$$\eta = -4 + \sqrt{15} = \{-1, 1, 6, 1, 6, 1, 6, \ldots\} \equiv \{-1, \overline{1, 6}\}, \tag{19}$$

where the over-line indicates the period which repeats *ad infinitum*.

Motivated by this strong result above we try to see whether the next bifurcations also have periodic representations in terms of continued fractions, i.e. whether they might also be reduced to quadratic irrationalities. Since the precision with which we know the additional parameters is not infinite, we first consider the continued fractions that one would obtain for ξ and η if we did not know that they were quadratic algebraic numbers:

$$\begin{aligned}
\xi \simeq -0.2679 &= \{-1, 1, 2, 1, 2, 1, 2, 1, 6, 1, 2, 2, 2, 1, 180749466, 1, 8, \ldots\}, \\
-0.267949 &= \{-1, 1, 2, 1, 2, 1, 2, 1, 2, 1, 2, 1, 5, 10, 2, 10, 38229, \ldots\}, \\
-0.26794919 &= \{-1, 1, 2, 1, 2, 1, 2, 1, 2, 1, 2, 1, 2, 1, 2, 1, 574, \ldots\}, \\
-0.2679491924 &= \{-1, 1, 2, 1, 2, 1, 2, 1, 2, 1, 2, 1, 2, 1, 2, 1, 2, \ldots\},
\end{aligned} \tag{20}$$

$$\begin{aligned}
\eta \simeq -0.1270 &= \{-1, 1, 6, 1, 6, 1, 15, 16166966871, 5, 1, 1, 2, 14, 1, 3, \ldots\}, \\
-0.127016 &= \{-1, 1, 6, 1, 6, 1, 7, 31, 2, 1, 1, 1, 1785679, 1, 1, 1, 1, \ldots\}, \\
-0.12701665 &= \{-1, 1, 6, 1, 6, 1, 6, 1, 6, 1, 13, 6, 3, 2, 2, 3, 23, \ldots\}, \\
-0.1270166537 &= \{-1, 1, 6, 1, 6, 1, 6, 1, 6, 1, 6, 1, 6, 1, 6, 1, 6, \ldots\}.
\end{aligned} \tag{21}$$

From these expansions one sees that for these two vertices a relatively small number of decimal places is already enough to recover the underlying periodicity of the quadratic numbers and to recover the numbers. The analogous expansion for the next vertex along v_1 gives

$$b_{1,3} \simeq -0.0970 = \{-1,1,9,3,4,3,2,157556662026,1,2,12,15,2,5,5,\ldots\},$$

$$-0.097031 = \{-1,1,9,3,3,1,2,1,2,3,2,6,1,3,1,30115,2,\ldots\},$$

$$-0.097031094 = \{-1,1,9,3,3,1,2,1,2,11,1,6,1,1,1,2,161,\ldots\},$$

$$-0.097031094104 = \{-1,1,9,3,3,1,2,1,2,11,1,8,1,6,3,9,2,\ldots\}. \qquad (22)$$

As is clear from these expansions, there is no detectable periodicity in Eq. (22). This absence of periodicity persists when we start expansions using all digits given in Table 3 and also when we compute the above expansions as long as the number of digits present in the original numbers permit. Absence of detectable periodicities occurs also for all other numbers in Tables 3 and 4, including the extrapolated values. Such finite expansions are obviously not a proof that they are not periodic, i.e. that they do not define quadratic irrationalities. But after experimenting numerically with several quadratic irrationalities we believe the detected absence of periodicity to be a overwhelming evidence in favor of irreducibility to quadratic irrationalities of all parameters characterizing higher bifurcations in Tables 3 and 4. Of course, to decide the nature of the irrationality one should simply investigate the minimal polynomials [2] defining vertices. The practical problem of implementing such approach, however, is that the determination of these polynomials from the equations of motion is not trivial computationally as the periodicity of the orbits increases more and more.

Periodic representations of algebraic numbers might be efficiently used to uncover an analytical relation between the coordinates of the point

$$p_{2,1}: \quad (a_{2,1}, b_{2,1}) = (1.23258\ldots, -0.28197\ldots), \qquad (23)$$

where the numbers are those for $n = 1$ in Table 4. To this end, notice that although the coordinates of $p_{1,1}$ and $p_{1,2}$ [as defined in Eqs. (1) and (15), respectively] involve quadratic irrationalities, the *ratios* of their coordinates, namely,

$$r_{1,1} \equiv \frac{a_{1,1}}{b_{1,1}} = -\frac{9}{2} \quad \text{and} \quad r_{1,2} \equiv \frac{a_{1,2}}{b_{1,2}} = -\frac{23}{2}, \qquad (24)$$

are rational numbers in both cases. Motivated by this fact we compute the continued fraction corresponding to the ratio between $a_{2,1}$ and $b_{2,1}$, obtaining

$$\frac{a_{2,1}}{b_{2,1}} = \{-5,1,1,1,\overline{2,3,1,6,1,3,2,1}\}, \qquad (25)$$

a periodic expansion. This periodic expansion allows us to obtain an exact analytical representation for $a_{2,1}/b_{2,1}$:

$$r_{2,1} \equiv \frac{a_{2,1}}{b_{2,1}} = -\frac{9+6\sqrt{2}}{4} \simeq -4.3713203\ldots \qquad (26)$$

which, when combined with the results from Ref. [1], yields

$$b_{2,1} = -\tfrac{1}{2} - \sqrt{2} + \tfrac{1}{2}\sqrt{5+4\sqrt{2}} \simeq -0.281971\ldots ,$$
$$a_{2,1} = r_{2,1} b_{2,1} \simeq 1.23258\ldots , \qquad (27)$$

defining analytically the location of the vertex $p_{2,1}$. We observe that although one knows expressions giving the analytical solutions of quartic polynomials, two popular commercial softwares with which we tried to factor the polynomial $81+1080a+3888a^2 - 4224a^3 + 256a^4$ returned such zeros in terms of those of the cubic resolvent instead of the considerably simpler analytical expression $a_{2,1}$ above.

Notice that all three analytical values of a and b defining vertices [which are given by Eqs. (1), (15) and (27)] obey the simple parameterization

$$a = r(\omega + \sqrt{\omega^2 - 1}), \qquad b = \omega + \sqrt{\omega^2 - 1}\,, \qquad (28)$$

and, since $bb^* = (\omega + \sqrt{\omega^2 - 1})(\omega - \sqrt{\omega^2 - 1}) = 1$, that b is a unit.

From the three analytical expressions for the vertices given above we see that while all four numbers which define the vertices $(a_{1,1}, b_{1,1})$ and $(a_{1,2}, b_{1,2})$ are *quadratic* irrationalities, the ratios $r_{1,1}$ and $r_{1,2}$ in Eq. (24) are simply *rational* numbers. We further see that while both $a_{2,1}$ and $b_{2,1}$ are *quartic* irrationalities, their ratio given in Eq. (26) is just a *quadratic* irrationality. From this it is very tempting now to conjecture that all similar ratios $r_{j,k}$ will have an algebraic degree which is half that of the $a_{j,k}$ and $b_{j,k}$ from which they originate. That such degree-halvings are related with the quadratic degree of the underlying equations of motion seems also to be a fair guess and an interesting question for further study.

We tried to determine the algebraic degree of additional ratios $r_{j,k}$ from the numbers given in Tables 3 and 4 but were not able to detect any other showing a quadratic signature and, therefore, believe them all to be irrationalities of higher degrees.

In order to obtain exact representations for additional vertices it would be of great help to have the aforementioned powerful result concerning quadratic irrationalities extended to situations involving higher irrationalities. A promising possibility in this direction seems to be the so-called Jacobi–Perron algorithm [26–31], among others [30]. The consideration of irrationalities of higher degrees, however, is a relatively complicated subject that will not be pursued here.

6. Conclusions

This paper considered nonlinear lattices generated by the coexistence of bifurcation cascades in the parameter space of dynamical systems. Bifurcations cascades generate an infinite number of families of "adjacent" algebraic varieties which overlap, i.e. co-exist, in certain regions. This overlap produces parameter lattices containing a 2D mesh of vertices defined by very specific numbers. We presented tables containing accurate numerical approximations of the coordinates of some of these vertices.

By considering the double limit of accumulation formed by the cascades starting with the lowest possible periods we obtained the first double accumulation point, the vertex $\mathscr{A}_{1,3}$, defined by Eq. (13), which is the unique point on its doubly infinite 2D lattice characterized by producing in phase space two different stable chaotic motions. It is possible to find infinitely many points similar to $\mathscr{A}_{1,3}$ but always for cascades other than the lowest possible ones, 1×2^m and 3×2^n.

Using the accurate parameters given in Tables 3 and 4 we attempted to determine the underlying number field in which such parameters are defined and to reconstruct their exact analytical form in the field. We presented analytical coordinates for three points for which the ratios $r_{j,k} \equiv a_{j,k}/b_{j,k}$ of their coordinates are at most quadratic numbers and argued that all remaining vertices should involve irrationalities higher than quadratic. Several open problems were also indicated. A particularly interesting one is the investigation of the evolution of basins of attraction along the varieties and vertices forming the lattice. Especially, to investigate the precise number-theoretic mechanism leading to transitions *smooth* $\rightleftharpoons$ *fractal* of basin boundaries as the periodicity increases without limit.

The present paper discussed vertices that are seen before and precisely at the "beginning" of chaos, i.e. when chaos appears for the first time while tuning parameters (from low to high periods). An interesting open problem is, of course, the number-theoretic characterization of what happens at the "last frontier" of chaos, where one finds phenomena and vertices analogous to those discussed in Refs. [10,32].

The characterization of the number-theoretic nature of parameter values defining points of multiple accumulations [like $\mathscr{A}_{1,3}$ here] is a quite interesting (and apparently not simple) problem. Both varieties u_∞ and v_∞ are at the "end" of infinite sequences of bifurcations characterized by *periodic* motions in phase space. Thus, all parameter values defining u_∞ and v_∞ cannot be algebraic, being therefore transcendental. Three relevant questions now are: (i) will a and b remain always multiples (or simple functions) of some basic unit as above? (ii) if so, how does the algebraic degree of their ratio varies along each variety v_j and/or u_k and between varieties? (iii) what is the specific number-theoretic characteristic that will tell us precisely *when* we finally "arrived" at points of accumulation and of multiple accumulations? Building on the discussions of Ref. [1] and on the evidence reported in this paper we offer the following tentative answers: a and b will remain multiples forever with their *ratios* being always given by algebraic irrationalities of degree lower than that of a and b, the only exception being the point of double accumulation for which not only a and b would be themselves transcendental, but its distinctive characteristic with respect to all other points of the lattice would be to have a *transcendental ratio* $r_{\infty,\infty}$. Of course, this is just an educated guess that remains to be demonstrated.

Acknowledgements

JG thanks Christine Schwartz and Michaela Weisskopf, Fernleihe der Zentralbibliothek, KFA Jülich, and Carla Bittencourt, Dipartimento di Fisica, Universitá degli Studi

"La Sapienza" di Roma, for the competent detective work of locating several articles from our incomplete (and partially wrong) references. He also thanks Peter Grassberger and Dietrich Wolf for fruitful discussions and for their kind interest in our work. MWB thanks FAPERGS for a post-doctoral fellowship. Both authors thank the Supercomputing Center of the University, CESUP-UFRGS, for granting access to the CRAY Y-MP 2E/232, where computations were done.

References

[1] J.A.C. Gallas, Units: remarkable points in dynamical systems, Physica A 222 (1995) 125–151.
[2] W. Narkiewicz, Elementary and Analytic Theory of Algebraic Numbers, 2nd Ed. (Springer, Berlin, 1990).
[3] B.N. Delone and D.K. Fadeev, The Theory of Irrationalities of the Third Degree, Transl. Math. Monographs, Vol. 10, 2nd printing (Amer. Math. Soc., Providence, RI, 1978).
[4] H.G. Grundman, Systems of fundamental units in cubic orders, J. Number Theory 50 (1995) 119–127.
[5] D.A. Buell and V. Ennola, On a parameterized family of quadratic and cubic fields, J. Number Theory 54 (1995) 134–148.
[6] M.W. Beims and J.A.C. Gallas, preprint (1996).
[7] P. Collet, J.-P. Eckmann and H. Koch, On universality for area-preserving maps of the plane, Physica D 3 (1981) 457–467; J.M. Greene, R.S. Mackay, F. Vivaldi and M.J. Feigenbaum, Universal behaviour in families of area-preserving maps, Physica D 3 (1981) 468–486; T. Bountis, Period doubling bifurcations and universality in conservative systems, Physica D 3 (1981) 577–589.
[8] F. Christiansen, P. Cvitanović and H.H. Rugh, The spectrum of the period-doubling operator in terms of cycles, J. Phys. A 23 (1990) L713–L717.
[9] J.A.C. Gallas, Structure of the parameter space of a ring cavity, Appl. Phys. B (Festschrift H. Walther), 60 (1995) S-203/S-213.
[10] J.A.C. Gallas, Structure of the parameter space of the Hénon map, Phys. Rev. Lett. 70 (1993) 2714–2717.
[11] P.J. Myrberg, Sur l'iteration des polynomes réels quadratiques, J. Math. Pures Appl. 41 (1962) 339–351.
[12] P.J. Myrberg, Iteration der reellen Polynome zweiten Grades, 3. Mitteilung, Ann. Acad. Sci. Fenn. Ser. A 336 (1963) 1–18; 2. Mitteilung 268 (1959) 1–13; 256 (1958) 1–10.
[13] B. Derrida, A. Gervois and Y. Pomeau, Universal metric properties of bifurcations of endomorphisms, J. Phys. A 12 (1979) 269–296.
[14] B. Derrida, A. Gervois and Y. Pomeau, Iteration of endomorphisms on the real axis and representation of numbers, Ann. Inst. H. Poincaré 29 (1978) 305–356.
[15] J.A.C. Gallas, Feigenbaum's constant for meromorphic functions, Int. J. Mod. Phys. C 3 (1992) 553–560.
[16] C. Mira, Chaotic Dynamics: From the 1D Endomorphism to the 2D Diffeomorphism (World Scientific, Singapore, 1987).
[17] S. Grossmann and S. Thomae, Invariant distributions and stationary correlation functions of 1D discrete processes, Z. Naturforsch. 32a (1977) 1353–1363.
[18] M.J. Feigenbaum, The universal metric properties of nonlinear transformations, J. Stat. Phys. 21 (1979) 669–706.
[19] P. Cvitanović, Universality in Chaos, 2nd Ed. (Adam Hilger, Bristol, 1989).
[20] W. de Melo and S. van Strien, One-Dimensional Dynamics (Springer, Berlin, 1992).
[21] J. Todd, Motivation for working in numerical analysis, in: Survey of Numerical Analysis, ed. J. Todd (McGraw-Hill, New York, 1962) pp. 5 and 86.
[22] A. Weil, Number Theory, An Approach through History, From Hammurapi to Legendre, Ch. III, Section XII Square roots and continued fractions (Birkhäuser, Boston, 1984).
[23] O. Perron, Die Lehre von der Kettenbrüchen, Vols. I and II 3rd Ed. (Teubner, Stuttgart, 1954).
[24] A. Khintchine, Kettenbrüche, 2nd Ed. (Teubner, Leipzig, 1956).
[25] W. Patz, Tafel der regelmässigen Kettenbrüche und ihrer vollständigen Quotienten für die Quadratwurzeln aus den natürlichen Zahlen von 1–10000 (Akademie-Verlag, Berlin, 1955).

[26] C.G.J. Jacobi, Allgemeine Theorie der kettenbruchähnlichen Algorithmen, in welchen jede Zahl aus drei vorhergehenden gebildet wird (Aus dem hinterlassenen Papieren von C.G.J. Jacobi mitgetheilt durch Herrn E. Heine), J. Reine Angew. Math. 69 (1868) 29–64.
[27] P. Bachmann, Zur Theorie von Jacobis Kettenbruch-Algorithmen, J. Reine Angew. Math. 75 (1873) 25–34.
[28] S. Pincherle, Saggio di una generalizzazione delle frazioni continue algebriche, Mem. Accad. Bologna 4 (1890) 513–538.
[29] O. Perron, Grundlage für eine Theorie des Jacobischen Kettenbruchalgorithmus, Math. Ann. 64 (1907) 1–76.
[30] L. Bernstein, The Jacobi–Perron Algorithm, its Theory and Application, Lecture Notes in Mathematics, Vol. 207 (Springer, Berlin, 1971).
[31] F. Schweiger, The Metrical Theory of the Jacobi–Perron Algorithm, Lecture Notes in Mathematics, Vol. 334 (Springer, Berlin, 1973).
[32] J.A.C. Gallas, C. Grebogi and J.A. Yorke, Vertices in parameter space: double crisis which destroy chaotic attractors, Phys. Rev. Lett. 71 (1993) 1359–1362.
[33] C. Simó, On the Hénon–Pomeau attractor, J. Stat. Phys. 21 (1979) 465–494.
[34] N. Metropolis, M.L. Stein and P.R. Stein, On infinite limit sets for transformations on the unit interval, J. Comb. Theory 15 (1973) 25–44.
[35] J. Milnor and W. Jhurston, On iterated maps of the interval, Lecture Notes in Mathematics, vol. 1342 (Springer, Berlin, 1988).
[36] R.M. May, Simple mathematical models with very complicated dynamics, Nature 261 (1976) 459–467.